J. Appl. Comput. Mech., 5(2) (2019) 344-354
DOI: 10.22055/JACM.2018.25142.1233

ISSN: 2383-4536
jacm.scu.ac.ir

M&MoCS
Shahid Chamran University of Ahvaz
Journal of Applied and Computational Mechanics

Research Paper

Traveling Waves of Some Symmetric Planar Flows of Non-Newtonian Fluids

Dongming Wei[1], Yupeng Shu[2]

[1] Department of Mathematics, School of Science and Technology, Nazarbayev University
53 Kabanbay Batyr Avenue, Astana, 01000, Kazakhstan

[2] Department of Mathematics, College of Sciences, the University of New Orleans
2000 Lakeshore Drive, New Orleans, LA 70148, USA

Received February 27 2018; Revised July 10 2018; Accepted for publication October 14 2018.
Corresponding author: Dongming Wei, dongming.wei@nu.edu.kz

Abstract. We present some variants of Burgers-type equations for incompressible and isothermal planar flow of viscous non-Newtonian fluids based on the Cross, the Carreau and the power-law rheology models, and on a symmetry assumption on the flow. We numerically solve the associated traveling wave equations by using industrial data and in order to validate the models we prove existence and uniqueness of solutions to the equations. We also provide numerical estimates of the shock thickness as well as the maximum stress associated with the traveling waves.

Keywords: Burgers-type equation; First-order implicit ODE; Existence and uniqueness of solutions; Numerical solutions.

1. Introduction

A viscous Newtonian fluid has a constant viscosity and a linear relation between the shear stress and the shear strain rate. Conversely, the viscosity of a non-Newtonian fluid varies with shear strain rate and the relationship between shear stress and shear strain is nonlinear [1], [2]. Newtonian fluids are ideal cases that we can see in real life, such as water and air etc. Most fluids can be classified as non-Newtonian fluids. For example, polymers, melted metals, human blood, paints, industrial mud and clay and most colloids, just to name a few. Many non-Newtonian fluids can be modeled by three rheological models: the Cross, the Carreau, and the power-law models [2]. The Cross and Carreau models cover the entire shear rate range, and they can be used to model the flows of liquid food and beverages [1], [3] and blood [4], [5]. The power-law model is applicable to many polymers as well as some liquid foods [4], [3]. In fact, these three rheology models are standard models adopted in chemical engineering, food processing, and petro-chemical engineering communities, see [3], [6], [7], [8], [9], [10], [11], and [2] for derivations and applications. Under some simple assumptions, we demonstrate that a class of equations of Burgers-type can be derived for incompressible, isothermal and symmetric non-Newtonian fluid planar flows. Table 1 lists mechanical and geometric properties in mathematical modeling.

It is well known that the Navier-Stokes equations for viscous planar flows are given by the following system [12], (Wei et al. 2011), [14], [15]:

$$\begin{cases} \rho(u_t + uu_x + vu_y) = \tau_{11,x} + \tau_{12,y} - p_x + f_1, \\ \rho(v_t + uv_x + vv_y) = \tau_{21,x} + \tau_{22,y} - p_y + f_2, \\ u_x + v_y = 0. \end{cases} \tag{1}$$

Here, we use $\vec{v} = (u, v)$ to denote the fluid velocity, ρ the density, $\tilde{\sigma} = \begin{pmatrix} \tau_{11} & \tau_{12} \\ \tau_{21} & \tau_{22} \end{pmatrix}$ the stress tensor, $\nabla p = (p_x, p_y)$ the pressure gradient, and $\vec{f} = (f_1, f_2)$ the external force.

Published online: March 18 2019

Table 1. Nomenclature

Symbol	Definition	Symbol	Definition
$\vec{f}$	External force	$\dot{\gamma}$	Shear rate
p	Pressure gradient	η	Apparent viscosity
p_x	Horizontal component of pressure gradient	η_0	Asymptotic value of η for zero shear rate η_0
p_y	Vertical component of pressure gradient	η_∞	Asymptotic value of η for infinite shear rate
u	Horizontal component of fluid velocity	κ	Time constant from reference resource
v	Vertical component of fluid velocity	$\bar{\kappa}$	Time constant
$\vec{v}$	Fluid velocity	ρ	Fluid density
x	Position in the horizontal direction	$\tau_{i,j}$	Element in the stress tensor where $i,j = 1,2$
y	Position in the vertical direction	$\varepsilon_{i,j}$	Element in the strain tensor where $i,j = 1,2$
α	Parameter in the Carreau-Yasuda model		

The strain tensor is denoted by $\tilde{\varepsilon} = \begin{pmatrix} \varepsilon_{11} & \varepsilon_{12} \\ \varepsilon_{21} & \varepsilon_{22} \end{pmatrix}$, where $\varepsilon_{11} = u_x$, $\varepsilon_{12} = \frac{1}{2}(u_y + v_x) = \varepsilon_{21}$, and $\varepsilon_{22} = v_y$. The subscripts t, x, and y are used to denote the corresponding partial derivatives, e.g., $v_x = \frac{\partial v}{\partial x}$, and the subscripts 1 and 2 are for vector components in the $x - direction$ of the $y - direction$ on the plane. The symmetry assumption we make is that $u(x,y,t) = u(x,t)$. Under this assumption and the incompressibility condition, we have $u_y = 0$, $u_x + v_y = 0$, $v = -yu_x + constant$, $\varepsilon_{21} = \varepsilon_{12} = \frac{1}{2}(u_y + v_x) = \frac{1}{2}v_x = -\frac{1}{2}yu_{xx}$, and $\varepsilon_{22} = v_y = -u_x$. In general, the constitutive rheology equation for viscous fluids is given in the following form:

$$\tilde{\sigma} = 2\eta(\dot{\gamma})\tilde{\varepsilon}, \tag{2}$$

where $\dot{\gamma}$ is the shear rate and the function $\eta(\dot{\gamma})$is the apparent viscosity. For planar flows, the relationship between stress and strain tensors is given by:

$$\tilde{\sigma} = \begin{pmatrix} \tau_{11} & \tau_{12} \\ \tau_{21} & \tau_{22} \end{pmatrix} = 2\eta(\dot{\gamma}) \begin{pmatrix} \varepsilon_{11} & \varepsilon_{12} \\ \varepsilon_{21} & \varepsilon_{22} \end{pmatrix}. \tag{3}$$

The shear rate for planar flow is given by $\dot{\gamma} = \left[2u_x^2 + 2v_y^2 + \frac{1}{2}(u_y + v_x)^2\right]^{\frac{1}{2}}$. For viscous Newtonian fluids, $2\eta = \mu = constant$, Equation (1) then reduces to:

$$\begin{cases} \rho(u_t + uu_x) = \dfrac{\mu}{2}u_{xx} - p_x + f_1, \\ \rho(v_t + uv_x + vv_y) = -\dfrac{\mu}{2}yu_{xx} - p_y + f_2, \end{cases} \tag{4}$$

under the symmetry and incompressibility assumptions. Suppose that the term $-p_x + f_1$ is very small and negligible and let $\nu = \frac{\mu}{\rho}$, then the first expression in Equation (4) is reduced to:

$$u_t + uu_x = \nu u_{xx}, \tag{5}$$

which is the well-known Burgers'equation for viscous Newtonian fluids [14], [16]. The inviscid counterpart of Equation (5) is:

$$u_t + uu_x = 0, \tag{6}$$

For non-Newtonian fluid flows η is not a constant, then we have:

$$\rho(u_t + uu_x) = 2[\eta(\dot{\gamma})u_x]_x - \eta(\dot{\gamma})u_{xx} - p_x + f_1. \tag{7}$$

Note that $|\dot{\gamma}| = 2u_x$ at $y = 0$, therefore for the power-law fluids, $\eta(\dot{\gamma}) = \mu|\dot{\gamma}|^{n-1}$, we have:

$$\rho(u_t + uu_x) = \hat{\mu}(|u_x|^{n-1}u_x)_x - p_x + f_1, \tag{8}$$

where $u = u(x,t)$, $\hat{\mu} = \mu 2^{(n-1)}\left(\frac{2n-1}{n}\right)$, $p_x = p_x(x,0,t)$, and $f_1 = f_1(x,0,t)$. Pressure-control flows are very important in studying microfluidic devices where the pressure can be controlled by inlet flow rate [17]. Based on this, we make the second assumption that the term $p_x + f_1$ can be considered to be very small and negligible. Therefore, we obtain the following Burgers-type equation

$$\rho(u_t + uu_x) = \hat{\mu}(|u_x|^{n-1}u_x)_x. \tag{9}$$

Some nonlinear equations, like Equation (9), have been studied extensively as mathematical models in [18], [19], [20], [16] and [21]. In particular, $\nu\left(\frac{u_x}{1+u_x^2}\right)_x$ was studied instead of $\hat{\mu}(|u_x|^{n-1}u_x)_x$ in [20], [22], and [19] in some Burgers-type equations. The analytic and numerical traveling wave solutions of equations like Equation (9) are given in [13], [14]. In the following, we denote $\tau_{11}(x,0,t)$ by σ and $\varepsilon_{11}(x,0,t) = u_x(x,0,t)$ by u_x. The assumption $u(x,y,t) = u(x,t)$ allows us to first solve for the flow velocity distribution on the $x - axis$ by solving the Burgers-type equation in $u(x,t)$ and then use $v(x,y,t) = -yu_x(x,t)$ for

the full velocity calculation. In Section 2, we derive a Burgers-type equation in $u(x,t)$ for the three non-Newtonian fluid models. Understanding the solutions of these equations can provide insight into the more complicated flow patterns for these important non-Newtonian fluids. The resulting ordinary differential equations (ODE) in $u(\xi)$, $\xi = x - ct$, from these partial differential equations (PDE) for traveling waves are all first-order implicit equations, and therefore the MATLAB built-in function ode15i() is used for computations of the numerical solutions. The use of the ode15i() function requires the values of $u_\xi(0)$ which are solved numerically by MATLAB's built-in function fzero before the numerical traveling wave solutions are calculated. In Section 3, Section 4, and Section 5, we solve the traveling wave equation to the Burgers-type equation, by using ode15i() for each of the three models respectively. The corresponding fluid velocity plots are also provided in the figures of these sections. Our numerical solutions and analysis indicate that the traveling wave solutions $u(\xi)$ for these nonlinear Burgers-type equations are all kink waves and the corresponding strains $u'(\xi)$ are solitons with various thickness of the transition layers. For illustration and comparison purposes, we have chosen experimental data from science and engineering literature as input parameters of the models for numerical computations. In Section 6, we use the Peano theorem with uniqueness in the implicit case to prove the existence and uniqueness of solutions to the nonlinear implicit first-order ODE and validate that the mathematical models are well-defined. In Section 7, we present numerical approximations of the thickness of transition layers and the corresponding maximum stress ε_{11} to compare the different behavior of the fluid flows predicted by the models.

2. A Variant of Burgers-type Equation for Some Non-Newtonian Fluids

For the incompressible, isothermal, viscous and symmetric planar fluid flows, the shear rate in Equation (2) is simplified into:

$$\dot{\gamma} = \sqrt{2\left[u_x^2 + (-u_x^2) + \frac{1}{2}(-yu_{xx})^2\right]} = \sqrt{4u_x^2 + \frac{1}{2}y^2u_x^2}. \tag{10}$$

Substituting Equation (10) into the first expression of Equation (1) and using $u_y = 0$, we have:

$$\rho(u_t + uu_x) = [2\eta(\dot{\gamma})u_x]_x - [\eta(\dot{\gamma})yu_{xx}]_y - p_x + f_1. \tag{11}$$

The right-hand side of Equation (11) can be rewritten as:

$$2\eta(\dot{\gamma})_x u_x + 2\eta(\dot{\gamma})u_{xx} - \eta(\dot{\gamma})_y yu_{xx} - p_x + f_1. \tag{12}$$

Since

$$\begin{cases} \eta(\dot{\gamma})_x = \dfrac{\eta'(\dot{\gamma})}{2\dot{\gamma}}(8u_xu_{xx} + y^2u_{xx}u_{xxx}), \\ \eta(\dot{\gamma})_y = \dfrac{\eta'(\dot{\gamma})}{2\dot{\gamma}}yu_{xx}, \end{cases} \tag{13}$$

Equation (11) becomes

$$\rho(u_t + uu_x) = \frac{\eta'(\dot{\gamma})}{\dot{\gamma}}(8u_xu_{xx} + y^2u_{xx}u_{xxx})u_x + \eta(\dot{\gamma})u_{xx} - \frac{\eta'(\dot{\gamma})}{\dot{\gamma}}y^2u_{xx}^3 - p_x + f_1. \tag{14}$$

Substituting $y = 0$ into Equation (14) and assuming that $p_x(x,0,t) + f_1(x,0,t)$ is very small and negligible, we have:

$$\rho(u_t + uu_x) = 2\eta(\dot{\gamma})_x u_x + 2\eta(\dot{\gamma})u_{xx}. \tag{15}$$

Since $\dot{\gamma} = 2|u_x|$, Equation (15) becomes

$$\rho(u_t + uu_x) = [4\eta'(2|u_x|)|u_x| + \eta(2|u_x|)]u_{xx} \tag{16}$$

where $\eta'(\dot{\gamma}) = \frac{d\eta(\dot{\gamma})}{d\dot{\gamma}}$. Equation (15) can be used to determine the flow velocity u on the $x - axis$ and allows the other velocity component to be computed by using $v(x,y,t) = -yu(x,t)$. For the power-law rheology model $\eta(\dot{\gamma}) = \bar{\kappa}|\dot{\gamma}|^{n-1}$, then Equation (16) gives the power-law Burgers' equation (9), which reduces to the classical Burgers' equation (5) when $n = 1$, $\bar{\kappa} = 2\kappa$, and $\kappa = \mu$. For this reason, Equation (15) is called a variant of the generalized Burgers' equation for non-Newtonian fluids, by setting $p_x(x,0,t) + f_1(x,0,t) = 0$. The rheology equations considered in this work are: the Cross model, $\eta(\dot{\gamma}) = \eta_\infty + \frac{\eta_0 - \eta_\infty}{1+\bar{\kappa}|\dot{\gamma}|^n}$, the Carreau model, $\eta(\dot{\gamma}) = \eta_\infty + (\eta_0 - \eta_\infty)(1 + \bar{\kappa}|\dot{\gamma}|^2)^{\frac{n}{2}}$ and the power-law model, $\eta(\dot{\gamma}) = \bar{\kappa}|\dot{\gamma}|^{n-1}$, where η_0, η_∞, $\bar{\kappa}$, and n are material constants depending on the type of fluid, see, e.g. [3]. The resulting equations of these models from Equation (15) are called variants of the generalized Burgers' equations. We will show existence and uniqueness of the solution to the corresponding traveling wave equations and solve for these solutions numerically in the individual sections below.

3. Traveling Wave Solutions of the Cross Model

By using Equation (15) and the rheological equation for the Cross model, we have

$$\begin{cases} \rho(u_t + uu_x) = [2\eta(\dot{\gamma})u_x]_x, \\ \eta(u_x) = \eta_\infty + \dfrac{\eta_0 - \eta_\infty}{1 + \bar{\kappa}|u_x|^n}, \bar{\kappa} = (2\kappa)^n. \end{cases} \tag{17}$$

For traveling waves, we assume that $\xi = x - ct$ and $u(x,t) = u(x-ct) = u(\xi)$. Then $u_0(\xi) = \frac{du}{d\xi}$ yields $u_x = u'(\xi)$ and $u_t = -cu'(\xi)$. Thus Equation (17) in the traveling wave coordinate ξ yields:

$$-\rho c u' + \rho u u' = [2\bar{\eta}(u')u']' - \left[\int_0^{u'} \bar{\eta}(s)ds\right]' \tag{18}$$

We will use the following standard boundary conditions for the traveling waves:

$$\begin{cases} u(-\infty) = u_l, u'(-\infty) = 0, \\ u(\infty) = u_r, u'(\infty) = 0, \end{cases} \tag{19}$$

where u_r and u_l are positive constants satisfying $u_l > u_r$, see, e.g. [23]. Integrating Equation (18) gives:

$$2\bar{\eta}(u')u' - \int_0^{u'} \bar{\eta}(s)ds = \rho\left(\frac{u^2}{2} - cu\right) + c_1. \tag{20}$$

Applying boundary conditions in Equation (19) to Equation (20) yields:

$$\begin{cases} c_1 = \rho\dfrac{u_l u_r}{2}, \\ c_1 = \dfrac{u_l + u_r}{2}, \end{cases} \tag{21}$$

Substituting Equation (21) into Equation (20) yields:

$$2\bar{\eta}(u')u' - \int_0^{u'} \bar{\eta}(s)ds = \frac{\rho}{2}(u - u_l)(u - u_r). \tag{22}$$

Equation (22) is a first-order implicit ODE in the form $F(u'(\xi), u(\xi)) = 0$. For simplicity, we use boundary conditions $u_l = 1$ and $u_r = 0$, and assume that $u(0) = \frac{u_l + u_r}{2} = \frac{1}{2}$. We will apply the MATLAB built-in function ode15i() to solve it numerically. This implicit ODE solver requires not only the initial value $u(0)$, but also the initial first-order derivative $u'(0)$ as input data. A set of rheological data for the Cross model $\rho = 26, \eta_0 = 7.03, \eta_\infty = 8.46 \times 10^{-3}, n = 0.969$, and $\kappa = 0.195$, found in Table 1 from [4], is used to provide our first numerical example. The corresponding fluid is called Fluid A. With the data, Equation (22) becomes:

$$\frac{u^2}{2} - \frac{1}{2}u = \left(0.000325 + \frac{0.540}{1 + 0.402|u'|^{0.969}}\right)u' + \int_0^{u'} \left(\frac{-0.270}{1 + 0.402|u'|^{0.969}}\right)ds. \tag{23}$$

Substituting equation $\xi = 0$ and $u(0) = \frac{1}{2}$ into Equation (23) leads to:

$$-\frac{1}{8} = \left(0.000325 + \frac{0.540}{1+0.402|u'|^{0.969}}\right)u' + \int_0^{u'(0)} \left(\frac{-0.270}{1+0.402|u'|^{0.969}}\right)ds. \tag{24}$$

We need to solve Equation (24) for $u'(0)$ to use ode15(). Since $u'(0) < 0, |u'(0)| = -u'(0)$, then Equation (24) becomes:

$$\left\{0.000325 + \frac{0.540}{1 + 0.402[-u'(0)]^{0.969}}\right\}u'(0) + \int_0^{u'(0)} \left\{\frac{-0.270}{1 + 0.402[-s]^{0.969}}\right\}ds + \frac{1}{8} = 0. \tag{25}$$

Then, we set $x = -u'(0)$ and use the following definition for $f(x)$:

$$f(x) = -0.000325x - \frac{0.540x}{1 + 0.402x^{0.969}} + \int_0^{-x} \left\{\frac{-0.270}{1 + 0.402[-s]^{0.969}}\right\}ds + \frac{1}{8} = 0, \tag{26}$$

and finally substitute $y = -s$ and $ds = -dy$. When $s = 0, y = 0$; and when $s = -x, y = x$. The integral term becomes $\int_0^x \left(\frac{0.270}{1+0.402y^{0.969}}\right)dy$. Applying Taylor series expansion to the definite integral at $y = 1$, we have:

$$\begin{aligned} &\int_0^x \left(\frac{0.270}{1 + 0.402y^{0.969}}\right)dy \\ &\quad = 0.193(x-1) - 0.0267(x-1)^2 + 0.00523(x-1)^3 - 0.00122(x-1)^4 \\ &\quad + 0.00329(x-1)^5 + 0.226. \end{aligned} \tag{27}$$

Therefore, Equation (26) becomes:

$$f(x) = -0.000325x - \frac{0.540x}{1 + 0.402x^{0.969}} 0.193(x-1) - 0.0267(x-1)^2 + 0.00523(x-1)^3 - 0.00122(x-1)^4 + 0.00329(x-1)^5 + 0.351. \quad (28)$$

Next, we apply the fzero function in MATLAB, see e.g. [5] to solve $f(x) = 0$ in order to obtain $x = 0.671$ which gives $u'(0) = -0.671$. This now allows us to solve for $u(\xi)$ numerically from the implicit ODE in Equation (23). By using the numerical solutions, we plot the velocity component u, its derivative u' and the corresponding velocity vector field $\langle u, v \rangle$ and present the results in Fig. 1 (a), (b), and (c) respectively. Notice that the numerical solution of the axial velocity u is a kink wave while the corresponding axial strain u' is a soliton.

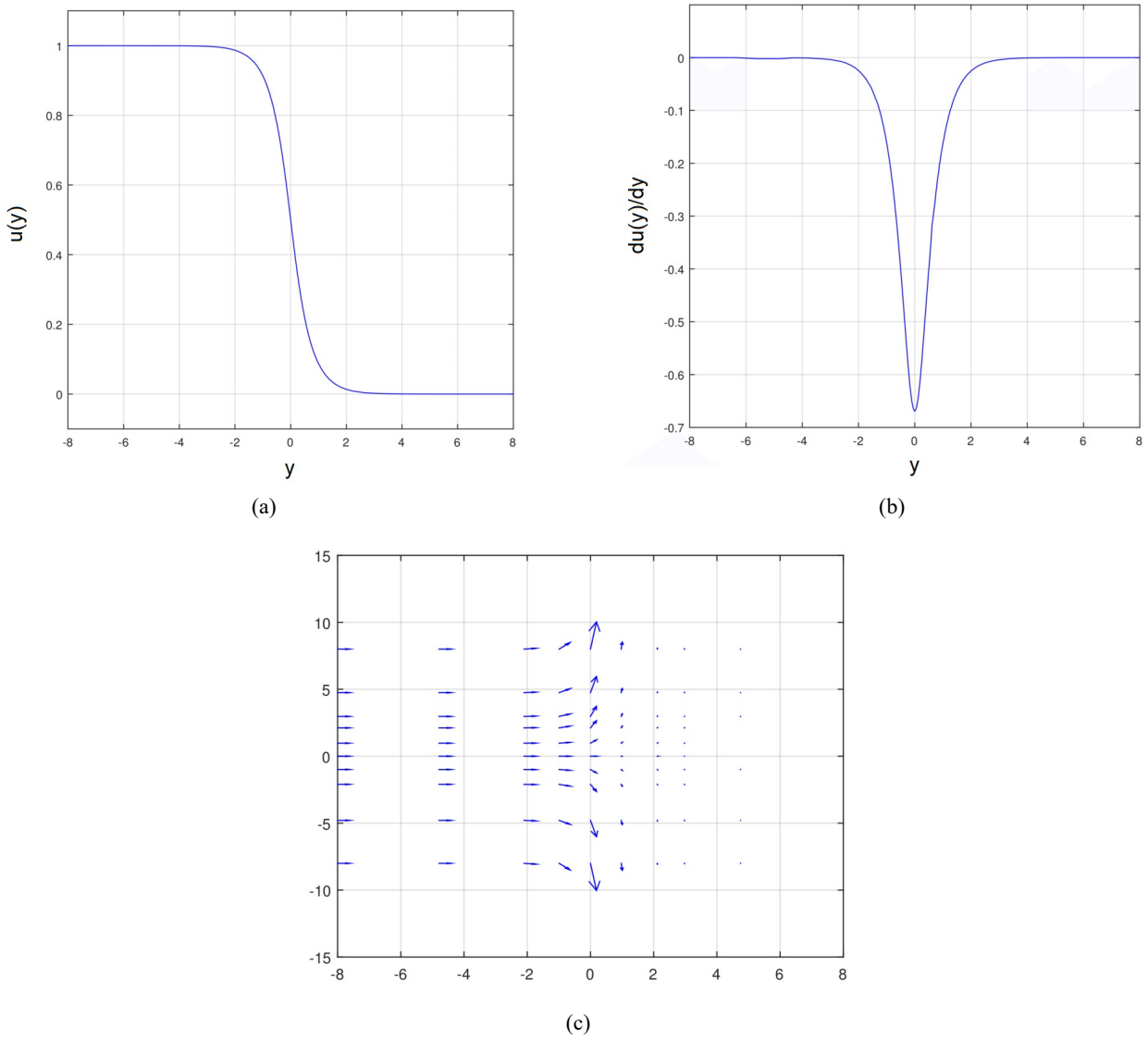

(a) (b)

(c)

Fig. 1. (a) The velocity component u (b) its derivative u' (c) the corresponding velocity vector field

4. Traveling Wave Solutions of the Carreau Model

Similarly, for the Carreau model we have:

$$\begin{cases} \rho(u_t + uu_x) = [2\eta(\dot{\gamma})u_x]_x \\ \eta(u_x) = \eta_\infty + (\eta_0 - \eta_\infty)(1 + \bar{\kappa}|u_x|^2)^{\frac{n-1}{2}}, \bar{\kappa} = 4\kappa^2, \end{cases} \quad (29)$$

with the boundary conditions:

$$\begin{cases} u(-\infty) = 1, u'(-\infty) = 0, \\ u(\infty) = 0, u'(\infty) = 0, \end{cases} \quad (30)$$

where u_r and u_l are positive constants. A set of data for fluid LLCF of the Carreau model is found in Table 2 from [24]: $\eta_0 = 0.454, \eta_\infty = 0.00689, n = 1.35, \kappa = 0.000554$, and $\rho \approx 1000$. The corresponding fluid is called Fluid B. Applying the procedure followed in Section 3 to the Carreau model, we have:

$$\frac{u^2}{2}-\frac{1}{2}u=[0.000454+0.00089422(1+0.000001227664|u'|^2)^{0.175}]u' + \int_0^{u'}[-0.00044711(1+0.000001227664|s|^2)^{0.175}]\,ds, \tag{31}$$

with $u(0)=\frac{1}{2}$, $u'(0)=-138.0863$. The power series expansion of the integral term in Equation (31) is also used for its evaluation. The corresponding numerical results are presented in Fig. 2 (a), (b), and (c) respectively.

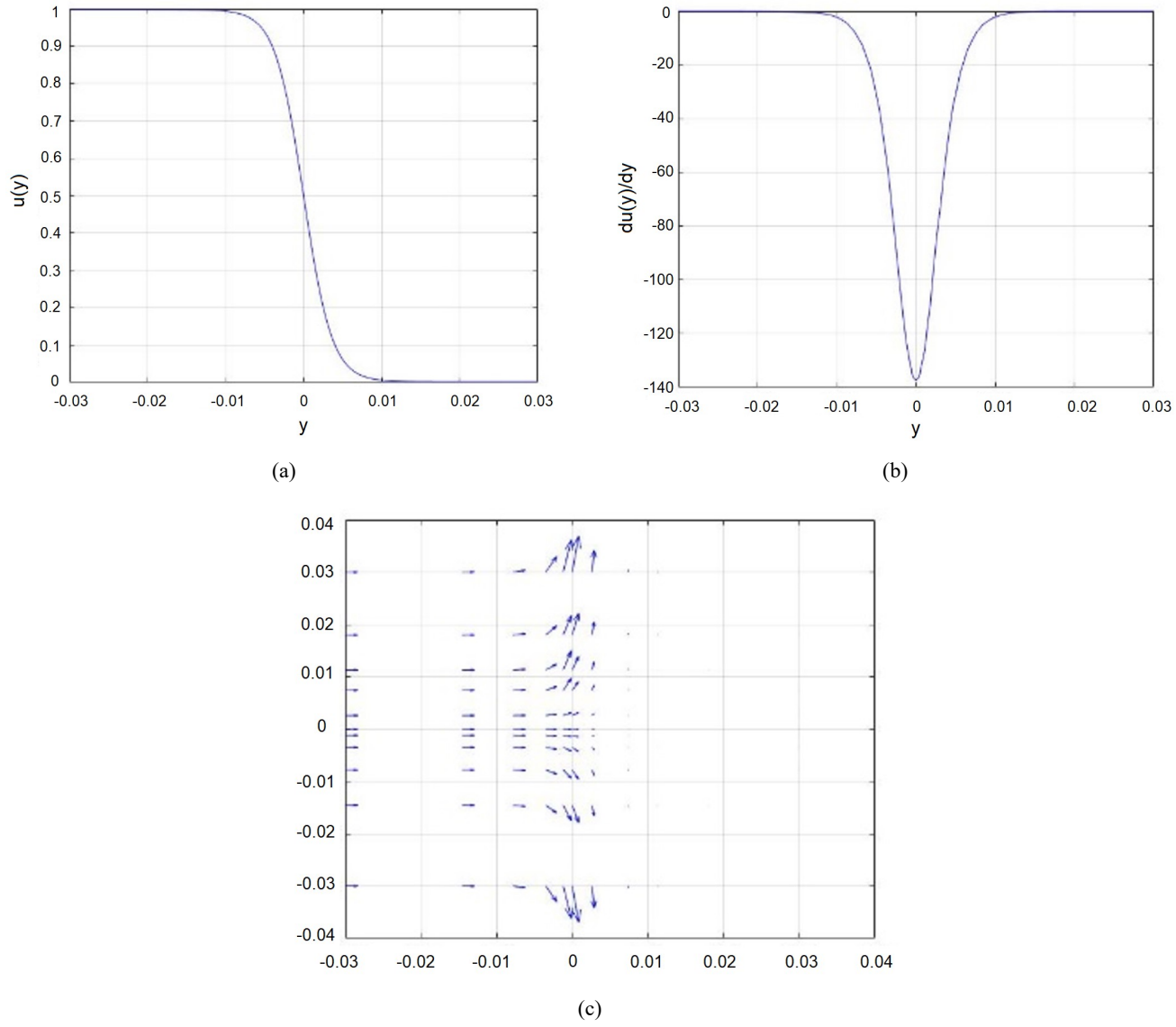

(a) (b)

(c)

Fig. 2. (a) The velocity component u (b) its derivative u' (c) the corresponding velocity vector field

5. Traveling Wave Solutions of the Power-law Model

Finally, for the power-law model, we use:

$$\begin{cases} \rho(u_t+uu_x)=[2\eta(\dot{\gamma})u_x]_x \\ \eta(u_x)=\bar{\kappa}|u_x|^{n-1}, \bar{\kappa}=\kappa\cdot 2^{n-1}, \end{cases} \tag{32}$$

with the boundary conditions:

$$\begin{cases} u(-\infty)=1, u'(-\infty)=0, \\ u(\infty)=0, u'(\infty)=0, \end{cases} \tag{33}$$

Selecting mayonnaise of the power-law rheology model in Table 10.4 from [25], we have 25℃, $\kappa=6.4$, and $n=0.55$. The density of mayonnaise of the power-law model can be calculated as the average of densities of the light and traditional mayonnaise as in [26], i.e., $\rho=955$. The corresponding fluid is called Fluid C. We have:

$$\frac{u^2}{2} - \frac{u}{2} = 0.00981|u'|^{-0.45}u' - 0.00491\int_0^{u'} |s|^{-0.45}ds \tag{34}$$

with $u(0) = \frac{1}{2}$, $u'(0) = -7995.485$. Note: there is no need to apply the power series expansion to the integral term of the power-law model because we can do the integration directly. The numerical results are provided in Fig. 3 (a), (b), and (c) respectively.

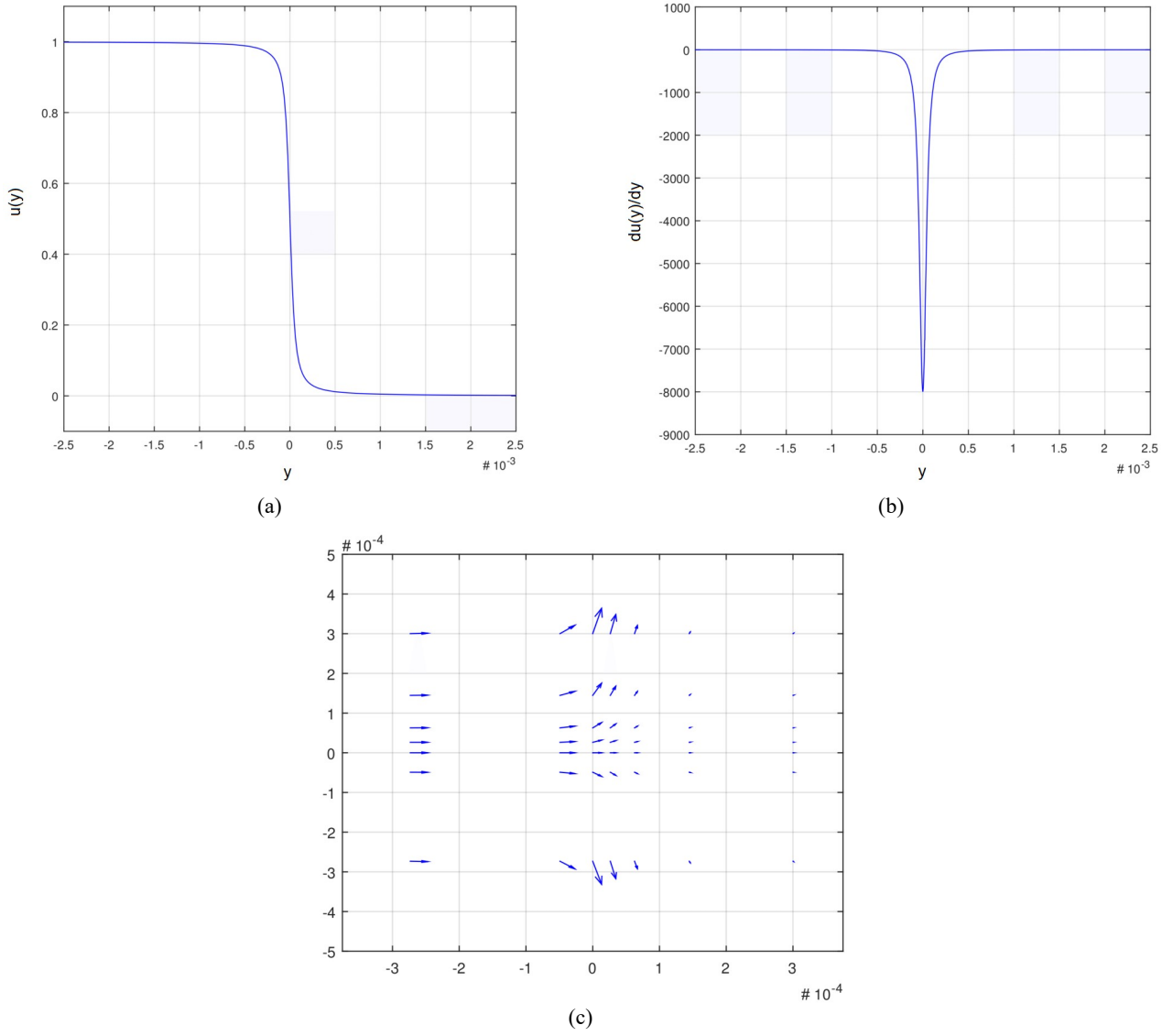

Fig. 3. (a) The velocity component u (b) its derivative u' (c) the corresponding velocity vector field

6. Existence and Uniqueness of Solutions to the Traveling Wave Equations

The Equations (17), (29), and (32) with the boundary conditions can be written in the following form:

$$\int_0^{u'(\xi)} \eta(s)ds - 2\eta\big(u'(\xi)\big)u' + au^2(\xi) + bu(\xi) + c = 0, \tag{35}$$

where $\eta(u'(\xi))$ is the apparent viscosity of the fluids and $a = \frac{\rho}{2}$, $b = -\rho\frac{u_l+u_r}{2}$, and $c = \frac{u_l u_r}{2}$ are the constants. This is a nonlinear implicit first-order integral-differential equation. To justify the validity of the mathematical models used for the numerical simulations in the previous sections, we shall apply the Peano theorem with uniqueness in the implicit case to the initial value problem:

$$\int_0^{u'(\xi)} \eta(s)ds - 2\eta\big(u'(\xi)\big)u' + au^2(\xi) + bu(\xi) + c = 0, \qquad u(0) = u_0 \tag{36}$$

for three fluid models with the data used in the last three sections. We shall apply Theorem 1 and Theorem 3 of Chapter 2 from [27] to show that for each of the three models, with the given boundary conditions and the coefficients, the problem (35) is well-defined. We shall also apply Theorem 3 of Chapter 3 from [27]; it follows that the uniqueness of solution can be obtained by

assuming the existence and continuity of $\frac{\partial F}{\partial u'}$ and $\frac{\partial F}{\partial u}$. To apply the Peano theorem and Theorem 3 of Chapter 3 from [27], let $F(u'(\xi), u(\xi), \xi)$ denote the left-hand side of the equation in (36). The theorem states that if the following conditions are satisfied, then the initial value problem (36) has a unique solution:
(1)$F(u'(\xi), u(\xi), \xi)$ of the three real variables $u'(\xi)$, $u(\xi)$, and ξ is defined and continuous on an open region U Of $\mathbb{R}^3$.
(2) all partial derivatives of F exist and are continuous on U.
(3) the initial value $(u'(0), u(0),0)$ is in U and it satisfies.

$$F(u'(0), u(0),0) = 0 \tag{37}$$

and

$$\frac{\partial F}{\partial u'}(u'(0), u(0),0) \neq 0. \tag{38}$$

We validate these conditions for the models below. For the Cross model, the existence and uniqueness of solutions are proved as follows. Substituting second expression of Equation (17) into Equation (35) produces:

$$F = \int_0^{u'} \left(\eta_\infty + \frac{\eta_0 - \eta_\infty}{1 + \bar{\kappa}|s|^n}\right) ds - 2\left(\eta_\infty + \frac{\eta_0 - \eta_\infty}{1 + \bar{\kappa}|u'|^n}\right) + \frac{\rho}{2}u^2 - \frac{\rho(u_l + u_r)}{2}u + \frac{u_l u_r}{2}. \tag{39}$$

Rearranging terms in Equation (39) gives:

$$F = \int_0^{u'} \left(\frac{\eta_0 - \eta_\infty}{1 + \bar{\kappa}|s|^n}\right) ds - \left[\eta_\infty + \frac{2(\eta_0 - \eta_\infty)}{1 + \bar{\kappa}|u'|^n}\right] + \frac{\rho}{2}u^2 - \frac{\rho(u_l + u_r)}{2}u + \frac{u_l u_r}{2}. \tag{40}$$

Taking partial derivative of Equation (40) with respect to u' gives:

$$\frac{\partial F}{\partial u'} = \frac{\eta_0 - \eta_\infty}{1 + \bar{\kappa}|s|^n} - \eta_\infty - 2(\eta_0 - \eta_\infty)\left[\frac{(1 + \bar{\kappa}|u'|^n) - u' \cdot n \cdot \bar{\kappa}|u'|^{n-1}(-1)}{(1 + \bar{\kappa}|u'|^n)^2}\right]. \tag{41}$$

Taking partial derivative of Equation (40) with respect to u gives:

$$\frac{\partial F}{\partial u} = \rho u - \frac{\rho(u_l + u_r)}{2}. \tag{42}$$

Since F is independent from ξ, then $\frac{\partial F}{\partial \xi} = 0$. As can be observed, all the first-order partial derivatives of F are continuously defined in the entire $\mathbb{R}^3$. It remains to check if $\frac{\partial F}{\partial u'} \neq 0$ at the data point for the numerical example in Section 3. For Fluid A, Equation (41) becomes:

$$\frac{\partial F}{\partial u'} = -\frac{0.00136|u'|^{1.938}}{(1 + 0.402|u'|^{0.969})^2} + \frac{2.638|u'|^{0.969}}{(+0.402|u'|^{0.969})^2} - \frac{7.03}{(1 + 0.402|u'|^{0.969})^2}. \tag{43}$$

At the data point $(u'(0), u(0),0) = \left(-0.671, \frac{1}{2}, 0\right)$, Equation (43) becomes:

$$\frac{\partial F}{\partial u'}\left(-0.671, \frac{1}{2}, 0\right) = -3.713 \neq 0. \tag{44}$$

So, this condition is also satisfied and therefore from the Peano theorem with uniqueness in the implicit case, it follows that our model example is well-defined. For the Carreau model, the conditions are checked as follows. Substituting the second expression from Equation (29) into Equation (35) yields:

$$F(u', u) = \int_0^{u'} \left[\eta_\infty + (\eta_0 - \eta_\infty)(1 + \bar{\kappa}|s|^2)^{\frac{n-1}{2}}\right] ds - 2\left[\eta_\infty + 2(\eta_0 - \eta_\infty)(1 + \bar{\kappa}|u'|^2)^{\frac{n-1}{2}}\right] u' + \frac{\rho}{2}u^2 - \frac{\rho(u_l + u_r)}{2}u + \frac{u_l u_r}{2}. \tag{45}$$

Rearranging terms in Equation (45) gives:

$$F(u', u) = \int_0^{u'} \left[(\eta_0 - \eta_\infty)(1 + \bar{\kappa}|s|^2)^{\frac{n-1}{2}}\right] ds - \left[\eta_\infty + 2(\eta_0 - \eta_\infty)(1 + \bar{\kappa}|u'|^2)^{\frac{n-1}{2}}\right] u' + \frac{\rho}{2}u^2 - \frac{\rho(u_l + u_r)}{2}u + \frac{u_l u_r}{2}. \tag{46}$$

Taking partial derivative of Equation (46) with respect to u' gives:

$$\frac{\partial F}{\partial u'} = -\eta_\infty - (\eta_0 - \eta_\infty)(1 + \bar{\kappa}|u'|^2)^{\frac{n-1}{2}} - (n-1)\bar{\kappa}|u'|^2(1 + \bar{\kappa}|u'|^2)^{\frac{n-3}{2}}. \tag{47}$$

Taking partial derivative of Equation (46) with respect to u gives:

$$\frac{\partial F}{\partial u} = \rho u - \frac{\rho(u_l + u_r)}{2}. \tag{48}$$

Substituting the data of Fluid B from Section 4 into Equation (47), we get:

$$\frac{\partial F}{\partial u'} = -0.00689 - 0.44711(1 + 0.000001227664|u'|^2)^{0.175} - \frac{0.0000004296824|u'|^2}{(1 + 0.000001227664|u'|^2)^{0.825}}. \tag{49}$$

At the point $(u'(0), u(0),0) = \left(-138.0863,\ \frac{1}{2}, 0\right)$, Equation (49) becomes:

$$\frac{\partial F}{\partial u'}\left(-138.0863, \frac{1}{2}, 0\right) \approx -0.464 \neq 0. \tag{50}$$

For the power-law model, substituting the second expression from Equation (32) into Equation (35) gives:

$$F(u', u) = \int_0^{u'} \bar{\kappa}|s|^{n-1} ds - 2[\bar{\kappa}|u'|^{n-1}]u' + \frac{\rho}{2}u^2 - \frac{\rho(u_l + u_r)}{2}u + \frac{u_l u_r}{2}. \tag{51}$$

Since $(u')^n$ is undefined when $u' < 0$, taking partial derivative of Equation (51) with respect to u' gives:

$$\frac{\partial F(u', u)}{\partial u'} = \frac{\bar{\kappa}}{n}(-n|u'|^{n-1}) - 2\bar{\kappa}[-(n-1)|u'|^{n-2}u' + |u'|^{n-1}]. \tag{52}$$

Since $-u' = |u'|$,

$$\frac{\partial F(u', u)}{\partial u'} = \bar{\kappa}|u'|^{n-1}(-1 + 2n). \tag{53}$$

For Fluid C from Section 5, $\bar{\kappa} = 0.00491$, $n = 0.55$, then Equation (53) becomes:

$$\frac{\partial F(u', u)}{\partial u'} = 0.000491|u'|^{-0.45} \neq 0. \tag{54}$$

At the point $(u'(0), u(0),0) = \left(-7995.485,\ \frac{1}{2}, 0\right)$, Equation (54) becomes:

$$\frac{\partial F}{\partial u'}\left(-7995.485, \frac{1}{2}, 0\right) = 0.00000860 \neq 0. \tag{55}$$

Taking partial derivative of Equation (51) with respect to u gives:

$$\frac{\partial F}{\partial u} = \rho u - \frac{\rho(u_l + u_r)}{2}. \tag{56}$$

For Fluid C from Section 5, $\rho = 955$, $u_l = 1$, and $u_r = 0$, Equation (56) becomes:

$$\frac{\partial F}{\partial u} = 955u - 477.5. \tag{57}$$

At the point $(u'(0), u(0),0) = \left(-7995.485,\ \frac{1}{2}, 0\right)$, Equation (57) becomes:

$$\frac{\partial F}{\partial u}\left(-7995.485, \frac{1}{2}, 0\right) = 0. \tag{58}$$

We have validated that all the conditions for the Peano theorem with uniqueness in the implicit case are satisfied for the three fluid models with the data used in the numerical examples above, and thus obtained the following:

Proposition 1. There exists a unique solution to the initial value problem (36) for each of the three fluid models with the data sets used in the three numerical examples.

7. The Thickness of the Transition Layers

The transition layer thickness or the shock thickness of the kink waves and the associated solitons can be computed by using the first order derivative $\frac{du}{d\xi}|_{\xi=0} = 0$ for the fluids. We use δ to denote the thickness of the transition layer and use the Taylor series expansion to yield:

$$u_l - u_r \approx u\left(-\frac{\delta}{2}\right) - u\left(\frac{\delta}{2}\right) = -\delta\frac{du}{d\xi}(0) + 0(\delta^2). \tag{59}$$

Therefore, we have $\delta = -\left[\frac{u_l - u_r}{u'(0)}\right] = -\frac{1}{u'(0)}$. For each of the three fluids, the maximum strain τ_{11} is calculated. This maximum strain $\tau_{11} = 2\eta\big(u'(0)\big)u'(0)$ occurs at the center of the kink wave which is also the center of the soliton. For each type of the fluids considered, we again use the same three industrial fluids Fluid A, Fluid B, and Fluid C as examples. The numerical results are listed in Table 2 for comparison.

Table 2. Thickness δ and Maximum Stress τ_{11}

Item	$u'(0)$	δ	τ_{11}
Fluid A	-0.671	1.489	-7.415
Fluid B	-138.0863	0.00724	-125.883
Fluid C	-7995.485	0.000125	-1313.139

It can be observed that even though traveling waves look similar in appearance for all the three fluid model examples, their transition layer thicknesses differ drastically and therefore the fluids behave quite differently.

8. Conclusion

In this paper, a Burgers-type equation for some common non-Newtonian fluid flows is derived from the planar Navier-Stokes equations under symmetry, isothermal and incompressibility conditions. By using this general equation and the Rheological equations of three basic models, three specific variants of Burgers-type equations and the associated traveling wave equations are derived. These traveling wave equations are first-order implicit integral-differential equations and they are numerically solved by using the MATLAB *ode15i* solver. Numerical examples are provided for three commonly encountered fluids with industrial rheological data. It is graphically demonstrated that the axial velocity profile for each fluid model is a kink wave while the corresponding strain wave is a soliton. The corresponding planar velocity profiles are also obtained. First-order approximations of the thickness of the transition layer, or thickness of the shocks, are also numerically computed. To provide a validation of the mathematical model, existence and uniqueness of the solutions to each of the three traveling wave equations with initial conditions are proved by using the Peano theorem with uniqueness in the implicit case.

Conflict of Interest

The author(s) declared no potential conflicts of interest with respect to the research, authorship and publication of this article.

Funding

The author(s) received no financial support for the research, authorship and publication of this article.

References

[1] Cross, M. M., Rheology of nonnewtonian fluids - a new flow equation for pseudoplastic systems, *J. Colloid Sci.* 20(5) (1965) 417-437.
[2] Fung, Y. C., *Biomechanics: Mechanical Properties of Living Tissues*, Springer, 1993.
[3] Steffe, J. F., *Rheological Methods in Food Process Engineering* (2nd ed.), 2807 Still Valley Dr., East Lansing, MI 48823, USA: Freeman Press, 1996.
[4] Garakani, A. H. K. et al., Comparison between different models for rheological characterization of activated sludge, *Iran. J. Environ. Health. Sci. Eng.* 8(3) (2011) 255–264.
[5] Shibeshi, S. S. et al., The rheology of blood flow in a branched arterial system, *Appl. Rheol.* 15(6) (2005) 398–405.
[6] Tyn, M. U. et al., Partial Differential Equations for Scientists and Engineers (3 ed.), Upper Saddle River, New Jersey 07458, USA: Prentice-Hall, 1987.
[7] Ochoa, M. V., *Analysis of Drilling Fluid Rheology and Tool Joint Effect to Reduce Errors in Hydraulics Calculations*, Ph.D. Dissertation, Texas A & M Univ, 2006.
[8] Kythe, P. K., *An Introduction to Linear and Nonlinear finite Element Analysis: A Computational Approach*, Birkhauser Boston, 2004.
[9] Bird, R. B. et al., *Dynamics of Polymeric Liquids*, Volume 1 − 2. New York, USA: Wiley-Interscience, 1987.
[10] Gee, R. E. et al., Nonisothermal flow of viscous non-newtonian fluids, *Ind. Eng. Chem.* 49(6) (1957) 956–960.
[11] Wilkinson, W. L., *Non-Newtonian Fluids: Fluid Mechanics, Mixing and Heat Transfer*, New York,USA: Pergamon Press, 1960.
[12] Munson, B. R. et al., *Fundamentals of Fluid Mechanics* (7 ed.). Wiley, 2012.
[13] Wei, D. et al., Traveling wave solutions of burgers' equation for power-law non-newtonian flows, *Appl. Math. ENotes* 11 (2011) 133–138.
[14] Wei, D. et al., Traveling wave solutions of burgers' equation for gee-lyon fluid flows, *Appl. Math. E-Notes* 12 (2012) 129–135.
[15] White, F., Fluid Mechanics (7 ed.), McGraw-Hill Education, 2010.
[16] Camacho, V. et al., Traveling waves and shocks in a viscoelastic generalization of burgers' equation, *SIAM J. Appl. Math.* 68(5) (2008) 1316–1332.

[17] Olesen, L. H., *Computational fluid dynamics in microfluidic systems*, MS. Thesis, Philadelphia: Technical University of Denmark, 2003.
[18] Chertock, A. et al., On degenerate saturated-diffusion equations with convection, *Nonlinearity* 18(2) (2005) 609–630.
[19] Kurganov, A. et al., Effects of a saturating dissipation in burgers-type equations, *Commun. Pure Appl. Math.* 50 (1997) 753–771.
[20] Goodman, J. et al., Breakdown in burgers-type equations with saturating dissipation fluxes, *Nonlinearity* 12 (1999) 247–268.
[21] Rykov, Y. G., On the theory of discontinuous solutions to some strongly degenerate parabolic equations, *Russian Journal of Mathematical Physics* 7(3) (2001) 341-356.
[22] Kurganov, A. et al., On burgers-type equations with non-monotonic dissipative fluxes, *Commun. Pure Appl. Math.* 51 (1998) 443–473.
[23] Debnath, L., *Nonlinear Partial Differential Equations for Scientists and Engineers* (2 ed.), Birkhauser Boston, 2005.
[24] Escudier, M. P. et al., On the reproducibility of the rheology of shear-thinning liquids, *J. Non-Newtonian Fluid Mech.* 97 (2011) 99-124.
[25] Kythe, P. K., *An Introduction to Linear and Nonlinear Finite Element Analysis: A Computational Approach*, Birkhauser Boston, 2004.
[26] Charrondiere, U. R. et al., FAO/INFOODS Density Database Version 2.0. FAO. Food and Agriculture Organization of the United Nations Technical Workshop Report, Rome, Italy, 2002.
[27] Murray, F. J. et al., *Existence Theorems for Ordinary Differential Equations*, New York, USA: New York Univ. Press, 1954.